

ROTATION OF F₁-ATPase AND THE HINGE RESIDUES OF THE β SUBUNIT

TOMOKO MASAIKE¹, NORIYO MITOME¹, HIROYUKI NOJI², EIRO MUNHEYUKI¹, RYOHEI YASUDA²,
KAZUHIKO KINOSITA JR^{2,3} AND MASASUKE YOSHIDA^{1,2,*}

¹The Research Laboratory of Resources Utilization, Tokyo Institute of Technology, 4259 Nagatsuta, Yokohama 226-8503, Japan, ²CREST (Core Research for Evolutional Science and Technology) 'Genetic Programming' Team 13, Teikyo University Biotechnology Research Center 3F Nogawa 907, Miyamae-ku, Kawasaki 216-0001, Japan and ³Department of Physics, Faculty of Science and Technology, Keio University, Yokohama 223-8522, Japan

*Author for correspondence (e-mail: myoshida@res.titech.ac.jp)

Accepted 20 October; published on WWW 13 December 1999

Summary

Rotation of a motor protein, F₁-ATPase, was demonstrated using a unique single-molecule observation system. This paper reviews what has been clarified by this system and then focuses on the role of residues at the hinge region of the β subunit. We have visualised rotation of a single molecule of F₁-ATPase by attaching a fluorescent actin filament to the top of the γ subunit in the immobilised F₁-ATPase, thus settling a major controversy regarding the rotary catalysis. The rotation of the γ subunit was exclusively in one direction, as could be predicted by the crystal structure of bovine heart F₁-ATPase. Rotation at low ATP concentrations revealed that one revolution consists of three 120° steps, each fuelled by the binding of an ATP to the β subunit. The mean work done by a 120° step was approximately 80 pN nm, a value close to the free energy liberated by hydrolysis of one ATP molecule, implying nearly 100% efficiency of energy conversion. The torque is probably generated by the β subunit, which

undergoes large opening–closing domain motion upon binding of AT(D)P. We identified three hinge residues, βHis179, βGly180 and βGly181, whose peptide bond dihedral angles are drastically changed during domain motion. Simultaneous substitution of these residues with alanine resulted in nearly complete loss (99%) of ATPase activity. Single or double substitution of the two Gly residues did not abolish the ATPase activity. However, reflecting the shift of the equilibrium between the open and closed forms of the β subunit, single substitution caused changes in the propensity to generate the kinetically trapped Mg-ADP inhibited form: Gly180Ala enhanced the propensity and Gly181Ala abolished the propensity. In spite of these changes, the mean rotational torque was not changed significantly for any of the mutants.

Key words: F₁-ATPase, F₁F₀-ATP synthase, motor protein, rotation, single-molecule observation.

Introduction

F₁F₀-ATP synthase, the enzyme responsible for most of the ATP synthesis in the biological world, couples H⁺ translocation across membranes to synthesis/hydrolysis of ATP. It reversibly dissociates into a membrane part, F₀, a proton channel in itself, and a water-soluble part, F₁, an ATPase that is hence often called F₁-ATPase. The subunit composition of F₁ is α₃β₃γδε; the α₃β₃γ complex is the catalytic core that retains the major kinetic features of F₁-ATPase.

More than 10 years before the structure of F₁-ATPase was determined, Boyer proposed the binding change mechanism in which three conformations of the β subunit with different affinities for adenine nucleotide were assumed (Boyer and Kohlbrenner, 1981; Boyer, 1993). The input of energy changes the affinity of binding sites by cooperative conformational changes. The molecular model that best explained the binding change mechanism was the physical rotation of the γ subunit relative to a ring consisting of the α₃β₃ part. The crystal

structure of bovine heart mitochondrial F₁ (Abrahams et al., 1994) indeed showed that the β subunits are in three different states, as predicted by the binding change mechanism: the AMP–PNP bound form (β_{TP}), the ADP bound form (β_{DP}) and the empty form (β_E). Elaborate experiments by two groups indicated that the γ subunit rotates during catalysis (Duncan et al., 1995; Sabbert et al., 1996). However, other movements such as simple conformational changes could also explain the observations, and exclusive evidence for the rotation was sought. A decisive answer was provided by visualising the rotation through single-molecule imaging.

Observation of rotation

A novel system to detect rotation

We have established a novel system to detect rotation of a single F₁-ATPase molecule (Noji et al., 1997). A fluorescent actin filament was attached to the γ subunit of α₃β₃γ complex

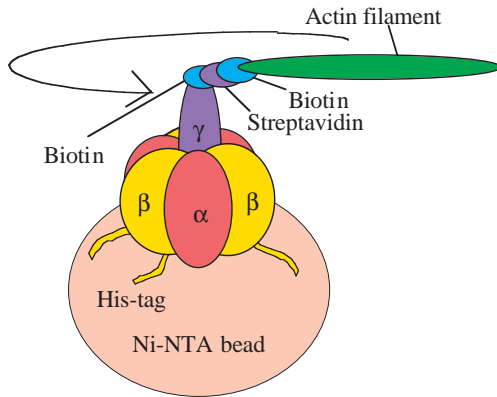


Fig. 1. The system used to observe the rotation of the γ subunit. For this assay system, mutations were introduced into the $\alpha_3\beta_3\gamma$ complex. A new cysteine was introduced into the γ subunit, to which biotin, streptavidin and biotinylated actin were attached in order. A sequence of 10 histidines at the N terminus of the β subunit (His-tag) immobilised the $\alpha_3\beta_3$ cylinder on a Ni^{2+} -nitrilotriacetic acid (Ni-NTA)-coated polystyrene bead.

from thermophilic *Bacillus* PS3, and the $\alpha_3\beta_3$ part was immobilised on a Ni^{2+} -nitrilotriacetic acid (Ni-NTA)-coated polystyrene bead (Fig. 1). Rotation of the actin filament in an anticlockwise direction was observed under a fluorescent microscope. The rotation was ATP-dependent and azide-sensitive (Noji et al., 1997). An actin filament that was attached to the ϵ subunit of $\alpha_3\beta_3\gamma\epsilon$ rotated in the same direction, and the ϵ subunit therefore also constitutes part of the rotor apparatus in F_1 -ATPase (Kato-Yamada et al., 1998).

Rotational steps at low ATP concentration

At ATP concentrations below 600nmol l^{-1} , the γ subunit rotated in steps of 120° , pausing at three dwell positions (Fig. 2) (Yasuda et al., 1998). Taking into account the pseudo-threefold symmetry of $\alpha_3\beta_3\gamma$ structure and that the binding of ATP to a catalytic site is the rate-limiting step under this condition, binding of ATP to an empty β subunit seems to initiate the stepping motion, and the work done during a step is fuelled by one ATP molecule. The plot of dwell time versus number of events was consistently exponential and was explained better by a one-ATP-per-step model than by a two-ATPs-per-step model (Yasuda et al., 1998). Thus, consumption of three ATP molecules for one rotation was confirmed. The possibility of smaller substeps is not excluded because of the limit of time resolution of our current system.

Torque and thermodynamic efficiency

Attachment of an actin filament to the γ subunit enabled not only visualisation of the rotation but also estimation of the torque generated by the rotation. Fig. 3 shows the dependence of the rotational speed of actin filaments on the length of the filaments. The mean torque was approximately 40pN nm ($4 \times 10^{-20}\text{J}$) irrespective of the load or the actin length, under conditions in which the free energy of

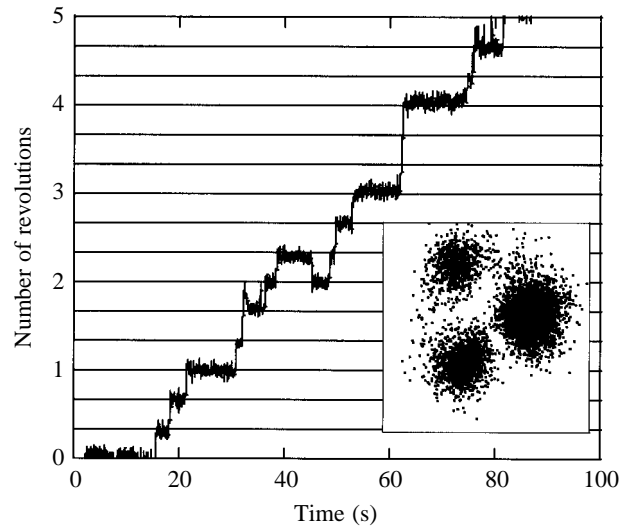


Fig. 2. Stepwise rotation at 20nmol l^{-1} ATP. The inset shows a trace of the centroid of the actin image. Actin length = $1.1\ \mu\text{m}$.

hydrolysis of one ATP molecule (ΔG) was 90 or 110pN nm . The work done by a one-third rotation was approximately 84pN nm ($40\text{pN nm} \times 2\pi/3$), indicating that the thermodynamic efficiency of conversion of the chemical energy of ATP hydrolysis to the kinetic energy of rotation is

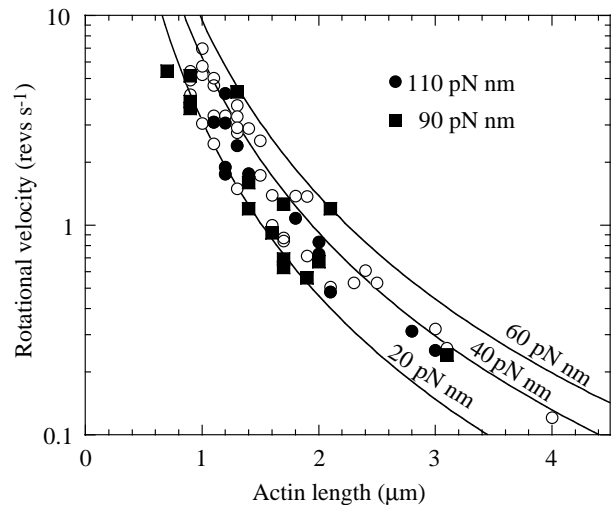


Fig. 3. Load-dependence of the rotational rate of the wild-type $\alpha_3\beta_3\gamma$ complex at $\Delta G=90$ or 110pN nm . ΔG is defined as (standard free energy change of ATP hydrolysis) $+RT \log_e[\text{ADP}][\text{P}_i]/[\text{ATP}]$, where R is the gas constant and T is absolute temperature. Open circles, measurements at $[\text{ATP}]=2\text{mmol l}^{-1}$ (because of the ATP-regenerating system, ΔG cannot be defined). Filled circles, measurements at $[\text{ATP}]=2\text{mmol l}^{-1}$, $[\text{ADP}]=10\ \mu\text{mol l}^{-1}$ and $[\text{P}_i]=0.1\text{mmol l}^{-1}$ ($\Delta G=110\text{pN nm}$). Filled squares, measurements at $[\text{ATP}]=2\text{mmol l}^{-1}$, $[\text{ADP}]=10\ \mu\text{mol l}^{-1}$ and $[\text{P}_i]=10\text{mmol l}^{-1}$ ($\Delta G=90\text{pN nm}$). The mean work done by a one-third rotation is 80pN nm , which gives approximately 100% efficiency of energy conversion. Theoretical lines give torque values of 40pN nm , 20pN nm and 60pN nm . $1\text{pN nm}=10^{-21}\text{J}$.

nearly 100%. This value contrasts with the reported values of efficiency of myosin/actin (20%) (Ishijima et al., 1995) and kinesin/microtubule (50%) (Svoboda et al., 1993). It is interesting to consider how the γ subunit would behave if ΔG were ≤ 80 pN nm. One possibility is that the rotation would slow down, keeping approximately 100% efficiency. Another possibility is that the rotational speed would not slow down, but that the enzyme would frequently fail in rotation even though ATP was hydrolysed, resulting in the overall consumption of two or more ATP molecules per step. To test which is the case is a challenge.

The hinge loop

The hinge for domain motion

Once rotation of the γ subunit had been established, the next problem was the mechanism of rotation. It is most likely that shifting the C-terminal domain of the β subunit towards the γ subunit triggers rotation of the γ subunit. For this kind of domain motion to occur, there should be a segment corresponding to a hinge connecting the two domains. For example, the crystal structures of myosin indicated that Gly457 and Ile455 (*Dictyostelium* myosin II) of the 'switch II' region constitute a hinge, and mutations of Gly457 caused the loss of both ATPase and motor activity (Fisher et al., 1995a,b; Smith and Rayment, 1996; Sasaki et al., 1998). Gly709 and Gly720 at the each end of the helix SH1 (chicken vertebrate smooth muscle myosin) are also identified as hinge residues. In the case of G-proteins, crystallisation and mutational analyses have revealed that Gly199 of the α subunit of bovine transducin is the hinge residue, and mutation of the residue resulted in the loss of the ability to activate the effector (Lee et al., 1992; Noel et al., 1993; Lambright et al., 1996). Thus, to describe the sequence of conformational changes of the β subunit of F_1 -ATPase, it is important to identify and characterise a hinge.

The hinge of the β subunit

To identify hinge residues in the β subunit, we compared the main-chain dihedral angles, ϕ and ψ (formed by four main-chain atoms starting from the carbonyl carbon of the previous residue and the amide nitrogen of the residue in question, respectively), of each residue in β_{DP} and β_E (refer to Introduction) of the crystal structure of bovine mitochondrial F_1 (Abrahams et al., 1994). Only five residues, Val162, Gly163, His179, Gly180 and Gly181 (numbering of *Bacillus* PS3), change either ϕ or ψ by more than 100° when the structure of β_{DP} is superimposed onto that of β_E . Val162 and Gly163 are residues in the Walker A motif, which is found at nucleotide binding sites in a variety of proteins, and are components of the P-loop (GGAGVGKT). The P-loop changes its conformation in response to nucleotide binding and hydrolysis, but this change is not a hinge-like motion. In contrast, Gly180 and Gly181 are located in the loop connecting helix B and strand β_4 (Fig. 4) (Abrahams et al., 1994). In β_{TP} and β_{DP} , His179 is also a component of the loop, but it is

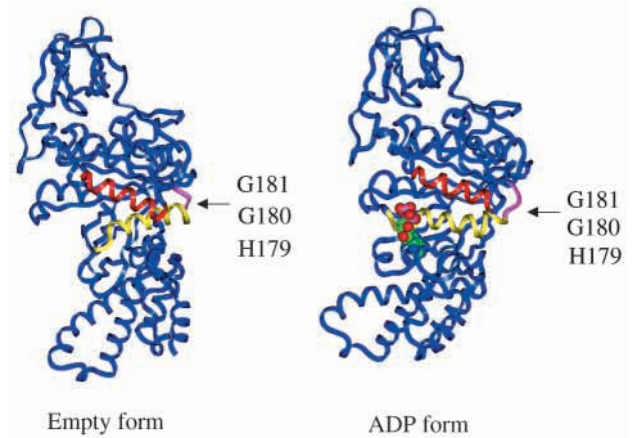


Fig. 4. Putative hinge loop of the β subunit in the empty form and the ADP form. The putative hinge loop is in pink, the Walker A sequence and helix B are in yellow, and helix C is in red. Taken from Abrahams et al. (1994) with permission.

involved in helix B in β_E . Helix B is preceded by the P-loop, and the strand β_4 is part of the 'wall' of parallel β sheet that surrounds the P-loop and helix B. The catalytic glutamic acid exists at the end of strand β_4 that is followed by helix C. As a whole, the catalytic site of the β subunit consists mostly the P-loop, helix B, strand β_4 , helix C and the wall of β sheet (Figs 4, 5) (Abrahams et al., 1994). When a nucleotide binds to the catalytic site, the N-terminal region of helix B is pulled up (Fig. 5), and this motion probably triggers swinging of the whole C-terminal helical domain. These three residues (β His179, β Gly180 and β Gly181) appear to allow the C-terminal domain to swing by changing their dihedral angles drastically. A large movement of His179 was already indicated by the report that the ^1H nuclear magnetic resonance peak of His179 of the free β subunit shifted downfield with increasing concentration of Mg-AMP-PNP (Tozawa et al., 1995). We replaced these residues with alanine and studied the characteristics of mutant $\alpha_3\beta_3\gamma$ complexes containing His179Ala, Gly180Ala and Gly181Ala.

Mg-ADP inhibited form

A brief scheme of ATP hydrolysis catalysed by F_1 -ATPase is shown in Fig. 6. It has been known that, when the product ADP is held in a stable manner at a catalytic site in the β subunit during ATP hydrolysis, the F_1 molecule becomes inactive. This inactive form is called the Mg-ADP inhibited form (Jault et al., 1995; Matsui et al., 1997). When the ATPase reaction is started by addition of ATP, the $\alpha_3\beta_3\gamma$ complex gets trapped in the Mg-ADP inhibited form in some probability and accumulates as turnover of the catalysis repeats, and the initial rate of ATP hydrolysis (initial ATPase activity) decreases towards an equilibrium rate (steady-state ATPase activity). The transition from initial activity to steady-state activity can be simulated by exponential fitting; the half-time of the transition for the wild-type $\alpha_3\beta_3\gamma$ complex was approximately 19 s under the conditions tested. The ratio of steady-state to initial

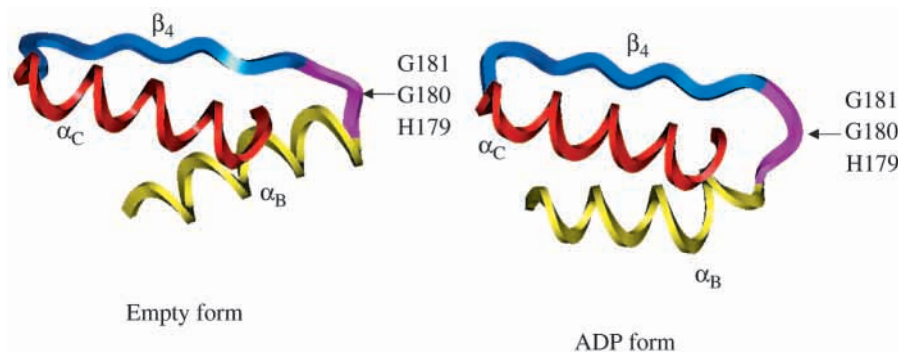


Fig. 5. Putative hinge loop and its motion. α_B , α helix B (yellow); α_C , α helix C (red); β_4 , β sheet 4 (light blue); the hinge loop is in pink. The nomenclature is taken from the crystal structure (see Abrahams et al., 1994).

activities was approximately 0.4. Because the precursor of the Mg-ADP inhibited form is thought to be an intermediate of the catalytic cycle, $F_1 \cdot \text{ADP}$, these values reflect the relative population of $F_1 \cdot \text{ADP}$ form during catalytic turnover.

ATPase activities of the mutants

Initial and steady-state ATPase activities of the mutants are shown in Fig. 7. In the case of the $\alpha_3\beta_3\gamma$ complex containing His179Ala, the initial ATPase activity did not change much, but the ratio of steady-state to initial activities decreased to 0.16. The half-time of the initial-to-steady-state transition was approximately 3.1 s. Thus, the propensity to fall into the Mg-ADP inhibited form increased. Interpretation of these changes is not easy because His179 becomes a part of helix B in the transition from β_{DP} (or β_{TP}) to β_E , as described above, and the replacement of His by Ala includes the loss of a hydrogen-bonding site for side chains of other residues. Therefore, His179Ala is not discussed in the next section. For the Gly180Ala mutant, the initial ATPase activity decreased to half that of the wild-type complex, but the decrease in the steady-state activity was more pronounced, to 7% of the wild-type value. The ratio of steady-state to initial activities was approximately 0.05, and the half-time of the initial-to-steady-state transition was approximately 3.4 s. In contrast, the $\alpha_3\beta_3\gamma$ complex containing Gly181Ala showed only very little time-dependent transition of activity; the initial ATPase activity was

not reduced, and no initial-to-steady-state transition was observed. Therefore, the Gly180Ala mutant demonstrates an enhanced propensity to fall into the Mg-ADP inhibited form, whereas the Gly181Ala mutant becomes resistant to Mg-ADP inhibition.

Changed stability of the closed form of the mutants

These observations regarding Gly180Ala and Gly181Ala can be explained by postulating a change in the stability of the closed form of the mutants (Fig. 8). At a saturating ATP concentration, the transition from open form 2 with an empty catalytic site to open form 1 with a bound ATP is very fast. In the case of Gly180Ala, the rapid initial-to-steady-state transition can be caused by the increased population of $F_1 \cdot \text{ADP}$, which results from stabilisation of the closed form. The stabilisation of the closed form leads to an increased activation energy for the transition from the closed form to

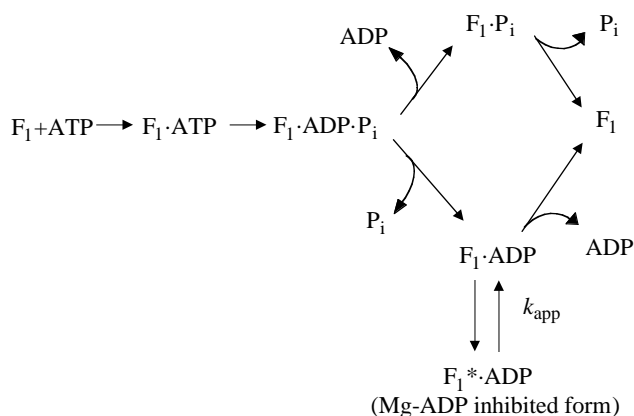


Fig. 6. A scheme of ATP hydrolysis catalysed by F_1 -ATPase. P_i , inorganic phosphate; k_{app} , apparent rate of inactivation.

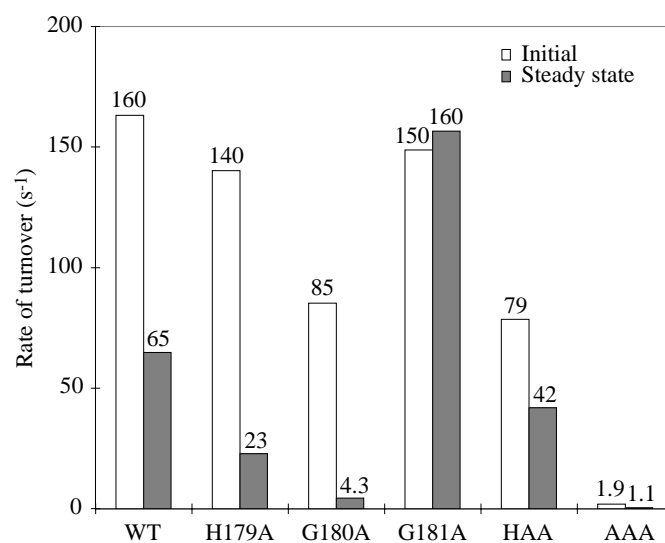


Fig. 7. ATPase activities of the mutants. ATPase activity was measured in Mops buffer: 10 mmol l⁻¹ Mops-KOH (pH 7.0), 50 mmol l⁻¹ KCl, 2 mmol l⁻¹ MgCl₂ and 2 mmol l⁻¹ ATP-Mg in an ATP-regenerating system. WT, wild type; H179A, $\alpha_3\beta(\text{His179Ala})_3\gamma$; G180A, $\alpha_3\beta(\text{Gly180Ala})_3\gamma$; G181A, $\alpha_3\beta(\text{Gly181Ala})_3\gamma$; HAA, $\alpha_3\beta(\text{Gly180Ala/Gly181Ala})_3\gamma$; AAA, $\alpha_3\beta(\text{His179Ala/Gly180Ala/Gly181Ala})_3\gamma$.

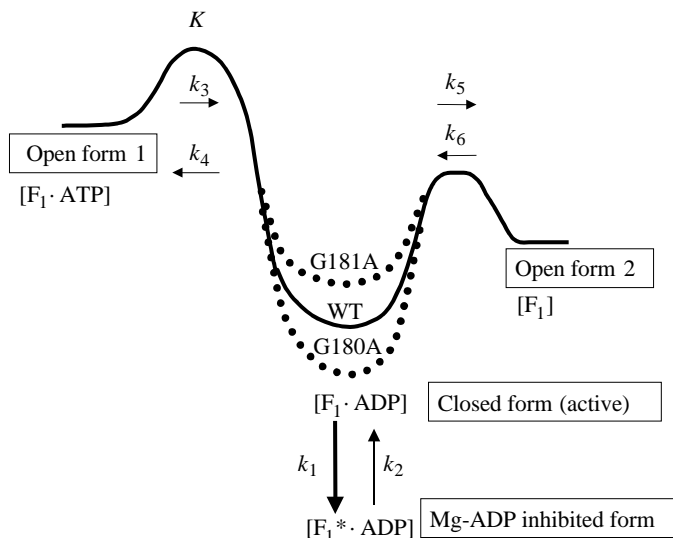


Fig. 8. A simple model to account for the observed changes in ATPase activity of the Gly mutants. We assume that F_1 and $F_1 \cdot \text{ATP}$ are in the open form and that $F_1 \cdot \text{ADP}$ and $F_1^* \cdot \text{ADP}$ are in the closed form. In addition, we also assume that the changes in the stability of $F_1 \cdot \text{ADP}$ caused the observed changes in the Gly mutants (shown schematically). As the onset of Mg-ADP inhibition is relatively slow compared with ATPase turnover, it can be assumed that F_1 , $F_1 \cdot \text{ATP}$ and $F_1 \cdot \text{ADP}$ are in rapid equilibrium. At a saturating ATP concentration and in the presence of an ATP-regenerating system, the amount of F_1 and the value of k_6 are negligible. Then, the apparent rate of inactivation due to inhibition by Mg-ADP (k_{app}) is expressed as $k_{\text{app}} = [k_1/(1+K)] + k_2$, where $K = [F_1 \cdot \text{ATP}]/[F_1 \cdot \text{ADP}]$, which is determined by the balance between k_3 , k_4 , k_5 and k_6 . The change in the relative stability of the open and closed forms directly affects K , k_5 and k_4 and hence the apparent rate of inactivation k_{app} and the initial ATPase activity (V_{max}). In the case of Gly180Ala, stabilisation of the closed form increases $[F_1 \cdot \text{ADP}]$, which results in a decrease in the value of K and an increase in the value of k_{app} . V_{max} is mainly determined by k_5 for this mutation, whereas it is determined mainly by k_3 in the wild type. In the case of Gly181Ala, destabilisation of the closed form decreases $[F_1 \cdot \text{ADP}]$, which results in a decrease in k_{app} . The rate-limiting step for Gly181Ala is k_3 , as for the wild type. The work done by the Gly180Ala and Gly181Ala mutants differs by less than 10% from that of the wild type concerning free energy change.

open form 2, which may result in the decreased initial ATPase activity of this mutant. In contrast, the closed form of the Gly181Ala mutant appears to be less stable, and $[F_1 \cdot \text{ADP}]$ may be lower than that in the wild-type complex. As a consequence, little or no Mg-ADP inhibited form is produced during catalysis, and the apparent rate of inactivation (k_{app}) decreases. The rate-limiting step in the catalytic cycle of this mutant may be the transition from open form 1 to the closed form, and the transition energy for this mutant is the same as that for the wild type, so that the initial ATPase activity is unchanged.

Ramachandran map of the hinge residues

The stability changes in the closed form of the mutant

complexes can be partly attributed to the steric stability of the mutated residues. The change in steric stability caused by the mutations discussed above was estimated in a Ramachandran map. The map was calculated for Gly-Gly, Ala-Gly and Gly-Ala peptides with various ϕ - ψ combinations (Fig. 9). The ϕ - ψ combination of Gly180 observed in the crystal structure of β_E is plotted in the area close to ‘outer limit’ of the energetically allowed region (Fig. 9A). Mutation of Gly180 to alanine seems to further destabilise this ϕ - ψ combination (Fig. 9B). Consequently, the open form (empty form) becomes less stable in this mutation, and $[F_1 \cdot \text{ADP}]$ increases. More Mg-ADP inhibited form is then generated. The situation is the reverse for the Gly181Ala mutant; the Ramachandran plot shows that Gly181 in the closed form (ADP form) takes the ϕ - ψ combination that is only allowed for glycine residue and that, when Gly181 is replaced by alanine, this ϕ - ψ combination becomes impossible (Fig. 9C,D). Thus, the Gly181Ala mutation destabilises the closed form (ADP form), the population of the closed form $[F_1 \cdot \text{ADP}]$ decreases, and the mutant complex becomes resistant to Mg-ADP inhibition (see legend to Fig. 8).

Double and triple mutants

The two single alanine mutations had opposite effects on the stability of the closed form. To investigate these effects in one molecule, the ATPase activity of a double Ala mutant (Gly180Ala/Gly181Ala, termed the HAA mutant) was measured (Fig. 7). This mutation resulted in approximately the same initial ATPase activity as that of the single alanine mutant Gly180Ala, but the steady-state ATPase activity was 65% of that of the wild type, contrasting with that of the single Gly180Ala mutant (7%). For this double mutant, there was an additional intermediate phase in the time course of ATPase activity besides the initial and steady-state phases. Therefore, resistance to Mg-ADP inhibition could not be defined by half-time of the initial-to-steady-state transition. However, the steady-state ATPase activity indicated that resistance to Mg-ADP inhibition was regained when the second mutation β Gly181Ala was introduced to the β Gly180Ala mutant. It is likely that destabilisation and stabilisation of $F_1 \cdot \text{ADP}$ occurred simultaneously, and the effects of both mutations seemed to be cancelled.

When we replaced all His-Gly-Gly residues with alanines (termed the AAA mutant), both initial and steady-state ATPase activity decreased drastically, to approximately 1% of those of the wild type (because of limits to the detection of the fast transition from initial state to steady state, the initial ATPase activity may include an error; Yasuda et al., 1998). In addition, the AAA mutant had a much faster apparent rate of inactivation than that of the wild type and even of the Gly180Ala mutant (data not shown). From these results, we can assume that stabilisation of the closed form was considerably enhanced, further impairing the opening-closing motion of the β subunit. Taken together, these results strongly indicate that the His-Gly-Gly loop contributes to the opening-closing motion of the β subunit.

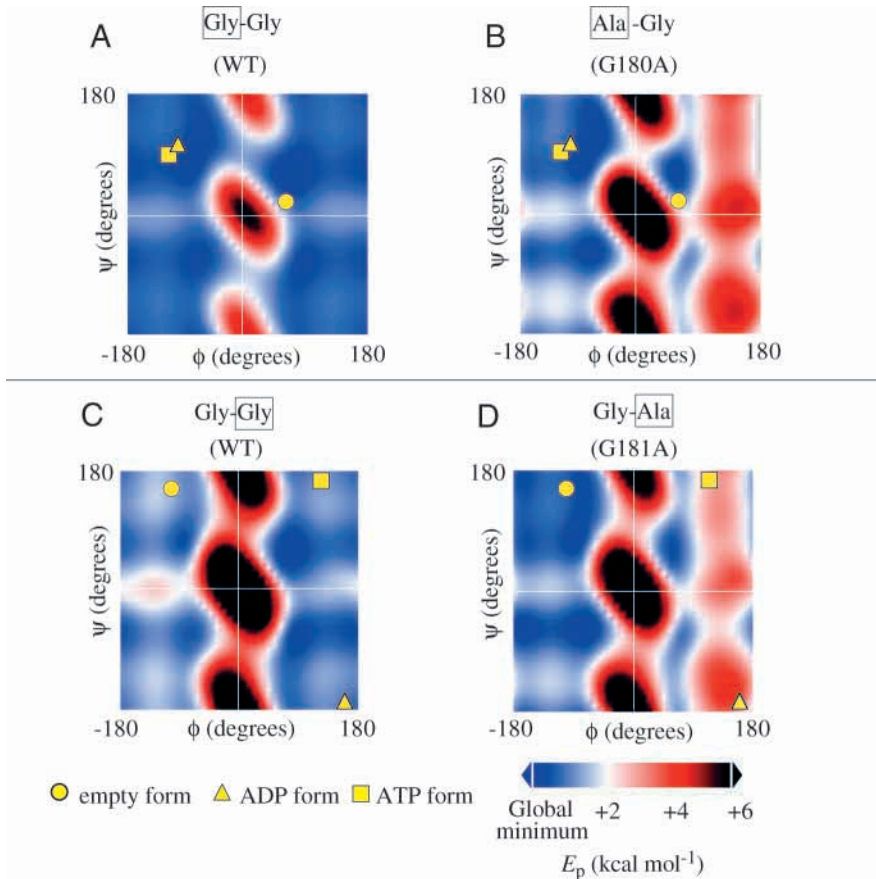


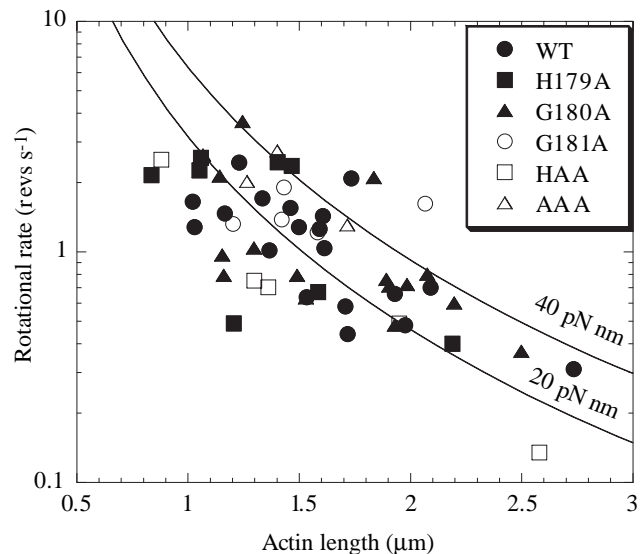
Fig. 9. Pairs of main-chain dihedral angles ϕ and ψ plotted on the Ramachandran map of the potential energy (E_p). Ramachandran maps were calculated using Discover3 (Molecular Simulations, USA) using the AMBER force field with the dielectric value of water. Each dipeptide is capped with an acetyl group and an NHCH_3 group. WT, wild type; G180A, $\alpha_3\beta(\text{Gly180Ala})_3\gamma$; G181A, $\alpha_3\beta(\text{Gly181Ala})_3\gamma$. The dihedral angles ϕ and ψ in each map indicate those of the boxed residue. Circles, empty form; triangles, ADP form; squares, ATP form.

Rotation of the hinge mutants

Rotation of these mutants was observed. As described in the previous section, the relative stability of the closed and open forms is changed by mutations at the hinge loop. Because we assume that the rotational work exerted by the hinge mutants corresponds to the potential difference between open form 1 and the closed form (Fig. 8), a change in the potential difference could lead to a change in the rotational torque. However, the γ subunit, for all the single alanine mutants, rotated with the same mean torque as that of the wild-type, irrespective of the actin length (Fig. 10). This is probably because the change in $[\text{F}_1\cdot\text{ADP}]$ affects the initial-to-steady-state transition rate in a more pronounced manner than it does the free energy of rotation. For example,

a 10-fold increase in $[\text{F}_1\cdot\text{ADP}]$ will result in a 10-fold increase in the initial-to-steady-state transition rate, while it will cause only a 10% increase in the potential difference (the work). In this case, torque should change by 10%, a value far smaller than the experimental error range of the present rotary assay system.

Fig. 10. Load-dependence of the rotational rate of the hinge mutants. The rotary assay was performed either in Mops buffer (10 mmol l^{-1} Mops-KOH, pH 7.0, 50 mmol l^{-1} KCl, 2 mmol l^{-1} MgCl_2 and 2 mmol l^{-1} Mg-ATP) or in potassium phosphate buffer (100 mmol l^{-1} potassium phosphate, 2 mmol l^{-1} MgCl_2 , pH 7.0) using an ATP-regenerating system. According to the rotary assay of the wild type, the torque is not affected by the difference between these two buffers (H. Noji, unpublished data). Mutation of the hinge loop did not affect the rotational torque. WT, wild type; H179A, $\alpha_3\beta(\text{His179Ala})_3\gamma$; G180A, $\alpha_3\beta(\text{Gly180Ala})_3\gamma$; G181A, $\alpha_3\beta(\text{Gly181Ala})_3\gamma$; HAA, $\alpha_3\beta(\text{Gly180Ala/Gly181Ala})_3\gamma$; AAA, $\alpha_3\beta(\text{His179Ala/Gly180Ala/Gly181Ala})_3\gamma$.



Perspectives

Our experimental system using an actin filament has enabled us to perform a direct ‘seeing is believing’ experiment. However, it is still to be improved. The population of actively rotating actin filaments is only a few per cent of the total filaments. This may be due to interference by other neighbouring F_1 molecules, to surface obstruction or to denaturation of F_1 molecules by immobilisation. Therefore, without extensive statistical analysis, it is difficult to distinguish pauses and stops that arise as natural characteristics of this enzyme from those originating from the experimental manipulations.

A simultaneous observation of rotation and ATP hydrolysis by a single molecule has not yet been successfully achieved. Therefore, we are obliged to estimate the rate of ATP consumption during rotation from measurements using unimmobilised F_1 molecules in a solution without load. At low ATP concentrations, because the rate-limiting step of the reaction is ATP binding, hydrolysis of one ATP molecule measured in a bulk solution roughly corresponds to one-third of a rotation of the filaments (Yasuda et al., 1998). However, at high ATP concentrations, the frictional load of filament rotation limits the speed of rotation, and the rate of ATP hydrolysis is probably suppressed accordingly. Measurement of the ATPase activity of a single F_1 molecule or observation of the rotation of the unloaded γ subunit is necessary to relate the timing of rotation directly to that of ATP hydrolysis. Experimental methods to measure both these in the same system are awaited.

Single-molecule experiments using F_1F_0 -ATP synthase must be performed to extend our understanding of its function as a holoenzyme. The ATP synthesis reaction catalysed by F_1F_0 -ATP synthase may not be merely the reverse of ATP hydrolysis by F_1 -ATPase. In the process of ATP synthesis, the source of energy for rotation is not the chemical energy of ATP hydrolysis, but H^+ flow through F_0 . In addition, the generation of the Mg-ADP inhibited form appears to be absent during ATP synthesis (Bald et al., 1998). Therefore, the rotation of the γ subunit during ATP synthesis needs to be confirmed. Moreover, classification of F_0 subunits into rotors and stators using the rotary assay will clarify the mechanism of F_1F_0 , as was achieved for F_1 .

A recent report that F_1F_0 undergoes contraction (Syroeshkin et al., 1998) is worth considering in exploring other movements required for ATP synthesis, although we have been unable to repeat the ‘sonic wave-driven ATP synthesis’ (N. Mitome, unpublished results). If this movement is essential for ATP synthesis, real-time detection of the up–down motion of a F_1F_0 molecule would be the next challenge.

We acknowledge Dr Tazashi Matsui for constructing the overexpression system of $TF_1 \alpha_3\beta_3\gamma$ and Dr Takayuki Nishizaka for providing carefully prepared actin filaments.

References

- Abrahams, J. P., Leslie, A. G. W., Lutter, R. and Walker, J. E. (1994). Structure at 2.8 Å resolution of F_1 -ATPase from bovine heart mitochondria. *Nature* **370**, 621–628.
- Bald, D., Amano, T., Muneyuki, E., Pitard, B., Rigaud, J.-L., Kruij, J., Hisabori, T., Yoshida, M. and Shibata, M. (1998). ATP synthesis by F_0F_1 -ATP synthase independent of noncatalytic nucleotide binding sites and insensitive to azide inhibition. *J. Biol. Chem.* **273**, 865–870.
- Boyer, P. D. (1993). The binding change mechanism for ATP synthase – some probabilities and possibilities. *Biochim. Biophys. Acta* **1140**, 215–250.
- Boyer, P. D. and Kohlbrenner, W. E. (1981). The present status of the binding-change mechanism and its relation to ATP formation by chloroplasts. In *Energy Coupling in Photosynthesis* (ed. B. Selman and S. Selman-Reiner), pp. 231–240. New York: North Holland Elsevier.
- Duncan, T. M., Bulygin, V. V., Zhou, Y., Hutcheon, M. L. and Cross, R. L. (1995). Rotation of subunits during catalysis by *Escherichia coli* F_1 -ATPase. *Proc. Natl. Acad. Sci. USA* **92**, 10964–10968.
- Fisher, A. J., Smith, C. A., Thoden, J., Smith, R., Sutoh, K., Holden, H. M. and Rayment, I. (1995a). X-ray structures of the myosin motor domain of *Dictyostelium discoideum* complexed with $MgADP \cdot BeFx$ and $MgADP \cdot AlF_4^-$. *Biochemistry* **34**, 8960–8972.
- Fisher, A. J., Smith, C. A., Thoden, J., Smith, R., Sutoh, K., Holden, H. M. and Rayment, I. (1995b). Structural studies of myosin:nucleotide complexes: a revised model for the molecular basis of muscle contraction. *Biophys. J.* **68**, 19–28.
- Ishijima, A., Harada, Y., Kojima, H., Funatsu, T., Higuchi, H. and Yanagida, T. (1995). Single-molecule analysis of the actomyosin motor using nano-manipulation. *Biochim. Biophys. Res. Commun.* **199**, 1057–1063.
- Jault, J. M., Matsui, T., Jault, F. M., Kaibara, C., Muneyuki, E., Yoshida, M., Kagawa, Y. and Allison, W. S. (1995). The $\alpha_3\beta_3\gamma$ complex of the F_1 -ATPase from the thermophilic *Bacillus* PS3 containing the α -D261N substitution fails to dissociate inhibitory MgADP from a catalytic site when ATP binds to noncatalytic sites. *Biochemistry* **34**, 16412–16418.
- Kato-Yamada, Y., Noji, H., Yasuda, R., Kinoshita, K. and Yoshida, M. (1998). Direct observation of the rotation of ϵ subunit in F_1 -ATPase. *J. Biol. Chem.* **273**, 19375–19377.
- Lambricht, D. G., Sondek, J., Bohm, A., Skiba, N. P., Hamm, H. E. and Sigler, P. B. (1996). The 2.0 Å crystal structure of a heterotrimeric G protein. *Nature* **379**, 311–319.
- Lee, E., Taussig, R. and Gilman, A. G. (1992). The G226A mutant of $G_{s\alpha}$ highlights the requirement for dissociation of G protein subunits. *J. Biol. Chem.* **267**, 1212–1218.
- Matsui, T., Muneyuki, E., Honda, M., Allison, W. S., Dou, C. and Yoshida, M. (1997). Catalytic activity of the $\alpha_3\beta_3\gamma$ complex of F_1 -ATPase without noncatalytic nucleotide binding site. *J. Biol. Chem.* **272**, 8215–8221.
- Noel, J. P., Hamm, H. E. and Sigler, P. B. (1993). The 2.2 Å crystal structure of transducin- α complexed with GTP γ S. *Nature* **366**, 654–662.
- Noji, H., Yasuda, R., Yoshida, M. and Kinoshita, K., Jr (1997). Direct observation of the rotation of F_1 -ATPase. *Nature* **386**, 299–302.
- Sabbert, D., Engelbrecht, S. and Junge, W. (1996). Intersubunit rotation in active F_1 -ATPase. *Nature* **381**, 623–625.
- Sasaki, N., Shimada, T. and Sutoh, K. (1998). Mutational analysis

- of the switch II loop of *Dictyostelium* myosin II. *J. Biol. Chem.* **273**, 20334–20340.
- Smith, C. A. and Rayment, I.** (1996). X-ray structure of the magnesium(II)-ADP-vanadate complex of the *Dictyostelium discoideum* myosin motor domain to 1.9 Å resolution. *Biochemistry* **35**, 5404–5417.
- Svoboda, K., Schmidt, C. F., Schnapp, B. J. and Block, S. M.** (1993). Direct observation of kinesin stepping by optical trapping interferometry. *Nature* **365**, 721–727.
- Syroeshkin, A. V., Bakeeva, L. E. and Cherepanov, D. A.** (1998). Contraction transition of F₁-F₀ ATPase during catalytic turnover. *Biochim. Biophys. Acta* **1409**, 59–71.
- Tozawa, K., Sekino, N., Soga, M., Yagi, H., Yoshida, M. and Akutsu, H.** (1995). Conformational dynamics monitored by His-179 and His-200 of isolated thermophilic F₁-ATPase β subunit which reside at the entrance of the conical tunnel in holoenzyme. *FEBS Lett.* **376**, 190–194.
- Yasuda, R., Noji, H., Kinoshita, K. and Yoshida, M.** (1998). F₁-ATPase is a highly efficient molecular motor that rotates with discrete 120° steps. *Cell* **93**, 1117–1124.